

MEDIUM RANGE ORDER IN NON-CRYSTALLINE MATERIALS

Mihai A. Popescu

National Institute of Materials Physics, Bucharest-Măgurele,
P.O. Box MG.7, Romania

The ordering in non-crystalline materials is shortly reviewed. The medium range order in covalent glasses is discussed with the special reference to As_2Se_3 glass. A new nanoparacrystallite model is advanced. The special ordering in metal glasses in relation to the effect of tensile load and thermal annealing relaxation is discussed. Finally, the anisotropy of the order in metal glasses and the medium range order in molten metallic alloys are discussed.

1. Introduction

In contrast to the crystalline state characterized by long range order (LRO), i.e. by correlations between the positions of every two atoms situated as far as possible one from another, the non-crystalline state is characterized by the absence of LRO. What remains is not a total disorder but a certain limited order called short range order (SRO), defined by the interatomic correlations in the first coordination spheres of an arbitrary atom, i.e. up to the maximum distance where the atomic forces are acting.

In many non-crystalline materials the order extends up to larger interatomic distances than those corresponding to SRO. On this basis a new type of order was defined: the medium range order (MRO) or the intermediate range order (IRO) [1,2,3].

MRO can be regarded as given by structural correlations in the range of 0.5 – 1 nm, in excess of that expected for an ideal Zachariasen – type continuous random network (CRN) characterized by a random dihedral angle distribution [4].

There is a great interest in the medium range order of covalent glasses and metal-metalloid disordered materials [5]. MRO plays an important role in the control of the physical properties of solid disordered materials. Nevertheless, a satisfactory explanation of the nature and properties of MRO for the most important classes of non-crystalline materials is still lacking.

2. The signature of the medium range order

The medium range order in non-crystalline materials do not give well defined spectroscopic pattern. The vibration spectra and, particularly, the Raman spectra can be in some circumstances sensible to some details in MRO [3].

The most powerful methods for the detection and investigation of MRO are those based on the diffraction of X-rays, electrons or neutrons. The main information regarding MRO is obtained from the diffraction patterns which exhibit either a pre-peak on the low angle side of the main diffraction maximum or a more or less developed first sharp diffraction peak (FSDP) or, even, a complex structure in the vicinity of FSDP, as recently reported by Baidakova et al.[6]. The atomo-electronic radial distribution function (RDF) calculated from the measured structure factor shows details at high distances which are related to MRO, but the structural information is an averaged one and, on the other hand, accurate RDF curves are rarely available.

In the X-ray diffraction curves the special features related to MRO are situated at low scattering wavevectors, while in the radial distribution functions, the high distances considered from an arbitrarily chosen atom carry the information on MRO.

Figs. 1 and 2 show the structure factors and the corresponding RDFs for amorphous ice prepared by deposition from water vapours on the substrates maintained at 77 K and at 10 K [7]. The MRO strongly differs in the two forms of a-ice, as can be seen, looking at the details on both type of curves. The preparation conditions are important factors in the developing of MRO, not only in a-ice but also in many other non-crystalline solids.

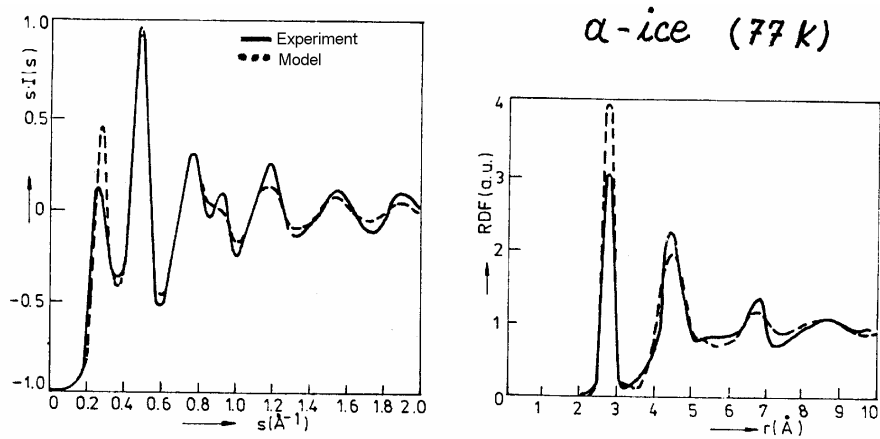


Fig. 1. The structure factor and the reduced (differential) radial distribution function of a-ice deposited and studied at 77 K (---) compared with those calculated from a structural model with 155 atoms developed by computer (—). The model contains a mixture of atom rings including 4-fold rings [8].

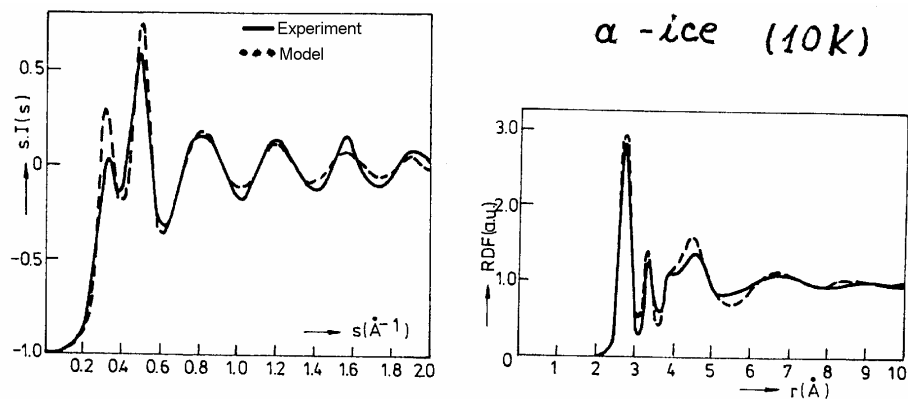


Fig. 2. The structure factor and the reduced (differential) radial distribution function of amorphous ice deposited and studied at 10 K (---) compared with those calculated from a structural model with 156 atoms (—). The model contains only even rings of atoms (6 and 8-fold rings) [8].

3. Medium range order in covalent glasses and the new nanoparacrystallite model

One of the largest class of covalent glasses is that of non-crystalline chalcogenides. The most studied members of this class consist in combinations or alloys of arsenic with the chalcogens (sulphur, selenium, tellurium).

We shall discuss in this section the As_2Se_3 glass. This is a stoichiometric glass and its crystalline form ($c\text{-As}_2\text{Se}_3$) is well known. The structure of the As_2Se_3 crystal consists of two-dimensional layers stacked along the crystallographic axis b . Each layer represents a system of interconnected twelve-member rings of alternating arsenic and selenium atoms [9]. The atoms are bonded only by heteropolar bonds according to the valency: three for arsenic and two for selenium atoms [10] (Fig. 3).

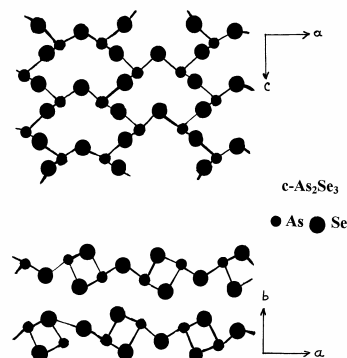


Fig. 3. The crystalline structure of an As_2Se_3 layer in $c\text{-As}_2\text{Se}_3$. The packing of the layers along the b -axis is also shown.

What happens when a crystal of As_2Se_3 is melted and the melt is, then, cooled at room temperature? The answer was given by the experiment: a glassy, vitreous or non-crystalline solid is obtained.

The structure of glassy, $g\text{-As}_2\text{Se}_3$, was thoroughly investigated along the last twenty five years. Fig. 4 shows the diffraction pattern of this material [11]. On the same plot are drawn the most intense diffraction lines characteristic to crystalline As_2Se_3 .

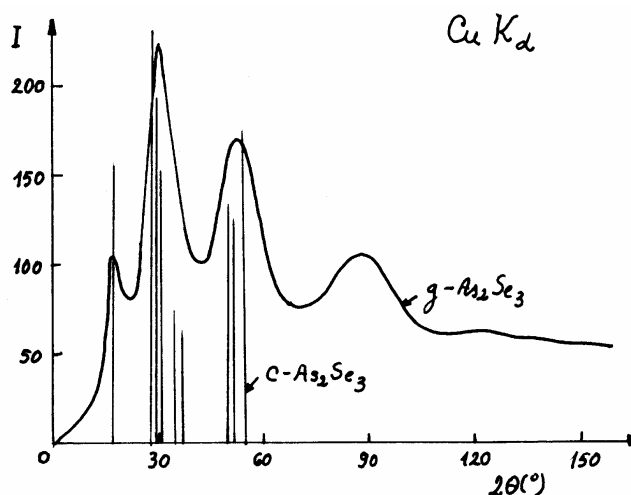


Fig. 4. The X-ray structure Factor of $g\text{-As}_2\text{Se}_3$. The first peak is FSDP and is located at $k = 1.27 \pm 0.004 \text{ \AA}^{-1}$.

It is tempting to conclude that the broad diffraction maxima in $g\text{-As}_2\text{Se}_3$ correspond to the average position of the group of diffraction lines of $c\text{-As}_2\text{Se}_3$. At a first glance, this means that, in this particular case, the microcrystalline theory for the structure of the glass should work. Nevertheless, if the fine details in Fig. 4 are observed, then one finds easily that a simple broadening of the crystalline diffraction peaks followed by their convolution, gives different positions and

intensities of the maxima in the diffraction pattern of $g\text{-As}_2\text{Se}_3$. Therefore the microcrystalline model must be discarded. In this case the medium range order in glassy arsenic selenide cannot be explained on the basis of limited size of the microcrystallites.

Before discussing a possible realistic model for the origin and the degree of extension of MRO in As_2Se_3 , let us follow the history of the problem.

Many scientists pointed out that the FSDP in the diffraction pattern of $g\text{-As}_2\text{Se}_3$ is significantly narrower than the other peaks and exhibits a peculiar behaviour. The characteristics of this peak (intensity, width and position on the scattering vector scale) is very sensitive to various physical parameters: temperature, pressure, annealing conditions, irradiation. There was shown that the variation of the FSDP intensity with the temperature and with the aggregation state (solid or molten state) is anomalous [12] in the sense that this peak increases reversibly with the temperature and becomes higher in the liquid state as opposite to the other peaks in the X-ray diffraction curve whose behaviour is normal (they decrease and become broader due to Debye – Waller factor). Fig. 5 shows this special feature.

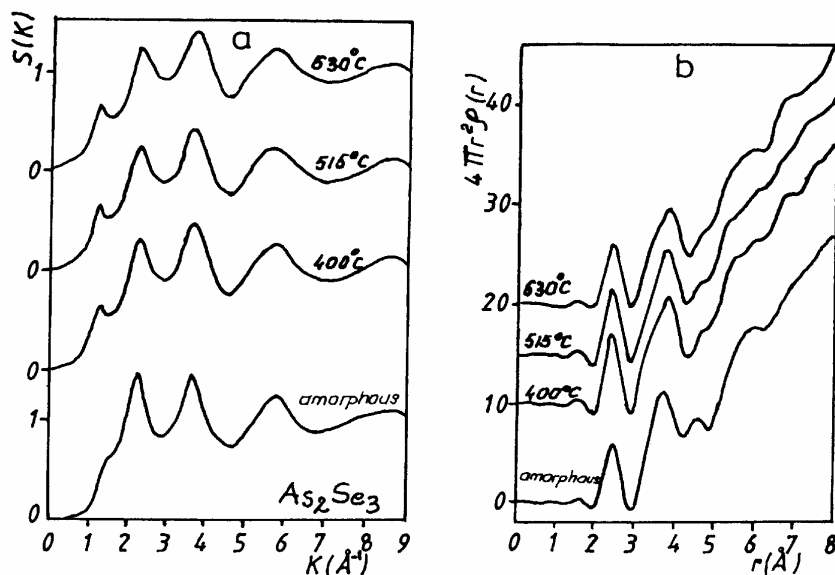


Fig. 5. The X-ray diffraction pattern of glassy As_2Se_3 at room temperature and in the liquid state at higher temperatures [13].

This strange behaviour challenged the scientists. Consequently new models for MRO emerged. The first one, supported by detailed calculations was the model with molecular clusters [14]. In this model the packing of As_4Se_6 molecules succeeded to reproduce the FSDP although with some arbitrariness in choosing the parameters. Thus, by changing the parameters as e.g. radius of cluster, packing density, etc. one can get any shape and intensity of the theoretical FSDP and a good fit to the experimental peak is ensured. Unfortunately new problems appear because the simultaneous fit to the other broad maxima in the diffraction curve is very difficult to get.

Later, Elliott [15] proposed an other model called void-based model or void correlation model, for the explanation of the FSDP, in general, without paying special attention to $g\text{-As}_2\text{Se}_3$. According to this model, the FSDP is a chemical order manifestation due to interstitial volume around cation-centred structural units. The calculated positions of FSDP for some covalent glasses (SiO_2 , GeO_2 , ZnCl_2 , GeS_2 , GeSe_2) agree well with the experimental ones and it is claimed that the anomalous dependencies of FSDP on pressure and temperature can be explained in the term of density effects. Nevertheless, this explanation tells nothing about the true nature of MRO when structural configurations are discussed.

In the old literature on chalcogenide glasses one remarks the structural model suggested by Vaipolin and Porai-Koshits [16], after a careful X-ray analysis of $g\text{-As}_2\text{Ch}_3$ (Ch=chalcogen) materials. According to this model, As_2Se_3 and the other arsenic chalcogenides consist of layer configurations similar to those found in crystals but strongly waved. Several groups of research support this model. Almost all the models developed up to day tried to explain mainly the FSDP, or the FSDP and the first main peak. They neglected, volens-nolens, the other details in the structure factor.

We have tried to show that the experimental data on $g\text{-As}_2\text{Se}_3$ and, possibly, on other covalent glasses, can be explained consistently on the basis of the paracrystallite concept developed by Hosemann [17].

Firstly, we would like to observe that in many chalcogenide glasses the broad maxima are located at the positions where intense diffraction peaks exist in the crystalline homologs. Fig. 6 shows, after Itoh [18], the cases of four arsenic selenide based glasses modified by Ag and Cu. It is noteworthy that neither the glassy nor the crystalline $\text{Ag}(\text{Cu})\text{-As}_x\text{Se}_y$ materials possess diffraction peaks at $2\Theta = 17^\circ$, ($\text{CuK}\alpha$ radiation) the position of FSDP in glassy As_2Se_3 . Therefore, the glasses show short range order and medium range order similar to those of the crystalline counterpart compounds.

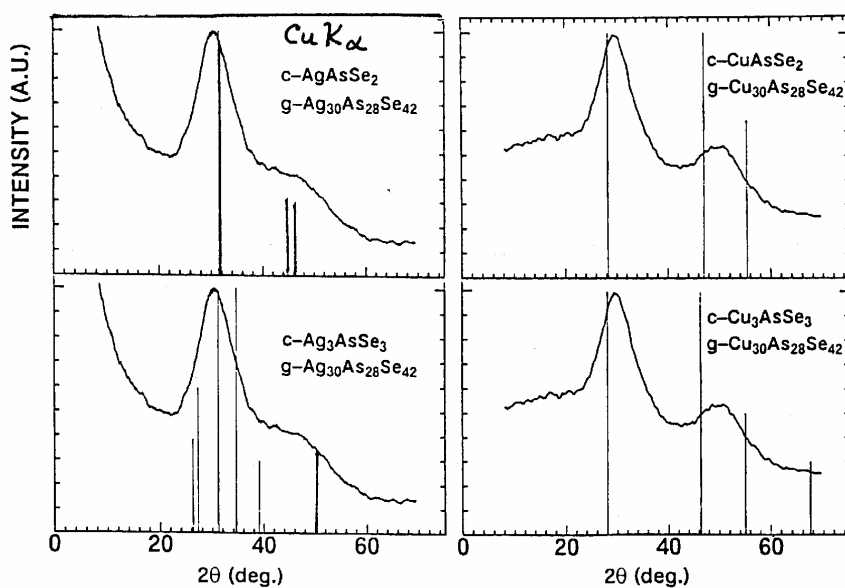


Fig. 6. X-ray diffraction patterns of glassy (g) and crystalline (c) $\text{Ag}(\text{Cu})\text{-As}_x\text{Se}_y$ glasses. Only intense peaks are shown in each crystalline diffraction patterns.

Now, let us look at the structure factor of the As_2Se_3 glasses from the point of view of the nanoparacrystallite theory. The diffraction pattern of As_2Se_3 glass shows peaks at the scattering wavevectors (k or s) which roughly corresponds to the higher order of diffraction of the first sharp diffraction peak. If these peaks can be ascribed to a single set (this hypothesis can be valid, indeed, for the first several maxima, because for larger scattering wave vectors the short range order effects dominate while the contribution of the main paracrystallite diffraction planes for higher diffraction order vanishes) then, it is possible to check the relation between the peak width and the diffraction order, as demonstrated by Hindeleh and Hosemann [19]. Indeed, as Fig. 7 shows, there exists a perfect linearity between the width of the diffraction maxima, δb , and the square of the quadratic sum, h^2 , of the Miller indices, for the basal paracrystallite plane (001) of the $c\text{-As}_2\text{Se}_3$. The dependency $\delta b \sim f(h^2)$ seems to be a strong argument in favour of the existence of paracrystallites as constitutive elements of the arsenic selenide glass.

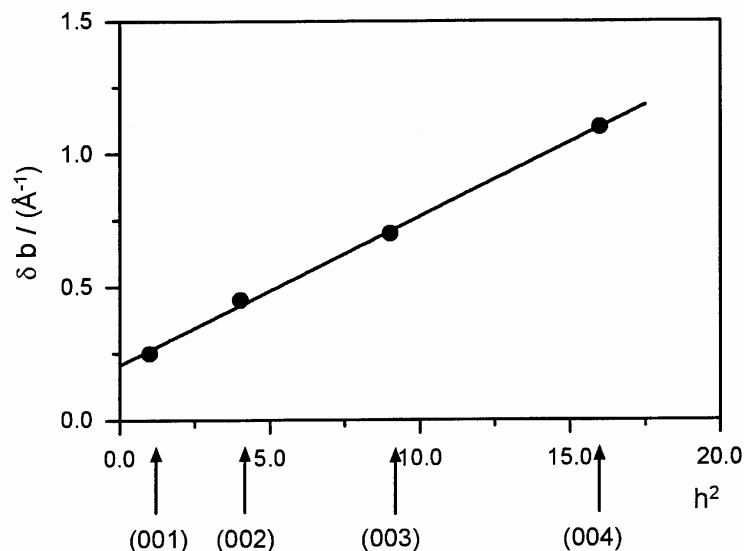


Fig. 7. The Hosemann plot for the paracrystallite structure in As_2Se_3 glass.

From the Hosemann graph one can get two important parameters. The intercept of the right line of the plot with the ordinate axis gives the value of $1/D$, where D is the average paracrystallite thickness measured normal to the basal paracrystalline plane. From the slope of the right line in the graph it is possible to calculate the paracrystallite distortion parameter, g , which is defined in the theory as the relative paracrystallite distance fluctuation, $g^2 = (d^2/d^2 - 1)^{1/2}$, where d is the average inter-plane spacing and d^2 is the mean square value of d . The mean paracrystallite thickness obtained for the g - As_2Se_3 is 2.98 nm. This value is in excellent agreement with the estimations reported in the literature. Taking into account the layered model, Leadbetter and Apling [20] have calculated a packing thickness of 2.0 – 2.2 nm, i.e. an average of four correlated layers. De Neufville et al. [21] have estimated a correlation range of 4 nm. The paracrystallite distortion parameter, g , determined from the Hoseman's graph is 0.16. This means that the nanoparacrystallites in As_2Se_3 show strong deviations from the ideal crystallite structure ($g=0$), but are well below the limit of the complete disappearance of any crystal-like feature ($g=1$).

The crystalline features in many glasses can be understood if one observes that during the amorphization process performed by applying high pressures, shock waves or by heavy particle irradiation, firstly vanish the crystallographic planes that are characterized by weak occupancy (low density). What remains, finally, is the backbone of the structural order, i.e. the best and strongest connected structural planes. In the case of quartz (α - SiO_2) the experiments have shown that the amorphous state can be reached by applying high pressures. Before amorphization, under hydrostatic as well as non-hydrostatic stress the material exhibits characteristic lamellar features [22]. The density of the lamellar "defects" increases with the pressure. The planar deformation features occur on rotational crystal planes and their dominant orientation is related to the peak stress. Below 12 GPa the dominant orientation is (0001). It is suggested that the amorphization results from the instability in the shear modulus in the (101n) planes.

In the case of chalcogenide glasses, which are characterized by atomic coordination 2 and 3, the basal layers lose the intrinsic order very easy during cooling of the melt but preserve the layer packing on the distance of the order of paracrystallite thickness parameter. The type of structural elements preserved in the glassy state seems to depend on the chemical composition of the material. Thus, there was firmly established that the dominant contribution to the FSDP in GeSe_2 glass is given by the Ge-Ge correlations [23]. This means that, primarily, the structural units based on tetrahedral germanium bonds are involved in the structural configuration responsible for MRO and this fact is

related to the better bonding and higher stability of the denser crystallographical planes based on packed germanium tetrahedra. The most stable structural planes of the corresponding crystalline phases are maintained in the disordered materials with ill defined packing and they give rise to MRO structural effects. The nanoparacrystallite theory which is well defined for the lamellar and fibrous structures seems to find in the chalcogenide glasses an appropriate working case.

In the frame of the nanoparacrystallite theory it is possible to explain all the characteristics and the complex behaviour of the FSDP while new parameters useful for glass characterization can be extracted. The high sensibility of the FSDP to various physical parameters can be explained by the existence of the basal paracrystalline configurations characterized by large packing distances. Bradaczek [24] has shown that the position and the intensity of the X-ray diffraction peaks change differently in every diffraction order as a function of the paracrystallite parameters. The FSDP which represents the first order diffraction peak in the paracrystalline model is, therefore, very sensible to the modifications of the paracrystalline configurations in glasses. The self-organization of the paracrystalline elements are governed by the long range forces that exists even in the liquid state at not too large temperatures.

4. Medium range order in glassy metallic alloys

The glassy metallic alloys or metglasses represent a large class of materials which contain metals (Fe, Co, Ni, Pd) combined with metalloids (Si, P, B), that can be obtained in non-crystalline state by rapid quenching of the melt (spin melting method and splat cooling procedures are used to this aim). Because the usual compositions involve metalloid and metallic elements in the proportion of 1:4, the metallic bond is dominant. The covalent component of the bonds is not negligible, but, moreover, is the essential factor for the stabilization of the glassy state.

In metglasses obtained as ribbons of various sizes were observed particular features related to more or less ordering at the atomic scale. On this basis it was possible to get deeper insight into the nature of MRO in these glasses.

Firstly we shall discuss the effect of a tensile load applied to the metglass on the atomic scale structure and, therefore, on the modification of SRO and MRO in such materials.

The effect of the tensile deformation on the structure of disordered Pd₄Si was studied by Matsumoto and Maddin [25,26]. They proposed a qualitative model describing the evolution of the structure with the deformation. The structural transformation suggested consists in an atomic scale change from a Bernal random close packed arrangement to a structure with crystalline islands which grow with the temperature, stress and time. Pampillo and Chen [27] revealed that in amorphous Pd_{77.5}Cu₆Si_{16.5} the compressive plastic deformation is highly inhomogeneous and it is supposed that some destruction of the SRO takes place. Masumoto and Maddin [28] found that the deformation stabilizes the internal structure of amorphous Pd₄Si and increases the crystallization temperature by 20-30°C. Masumoto et al. [29] have shown that cold rolling at room temperature produces a much more disordered structure in amorphous Pd-Si than is present in the as-quenched state. Using transmission electron microscopy and micro-electron diffraction, they proved that a cold rolled sample of Ni₇₅Si₈B₁₇ is heterogeneous. Bright bands whose diffraction pattern is different from that of the rest of the sample were observed. Waseda and Egami [30] studied the effect of cold rolling and isothermal creep on the structure of the splat-cooled glassy Pd₄Si and concluded that the structural change induced by deformation is quite distinct from the structural relaxation induced by annealing.

Popescu [31] studied the problem of structural relaxation under a tensile load applied to a metglass ribbon of composition Fe₈₀B₂₀. The X-ray diffracted intensity curves before applying a tensile load (as-quenched state), after mechanical deformation (stretched state) and after one day of relaxation (relaxed state) are shown in Fig. 8.

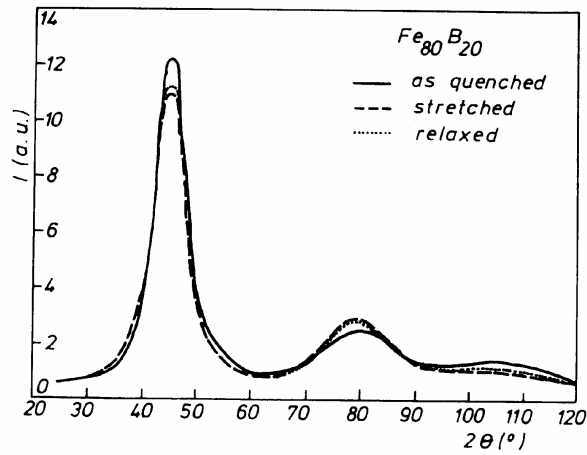


Fig. 8. The X-ray diffracted intensity patterns of glassy $\text{Fe}_{80}\text{B}_{20}$ ribbon.

The deformation induces a significant decrease of the height of the first diffraction peak, while the second peak increases and the following broader peak diminishes its intensity. The relaxation results in slight modifications in the X-ray pattern, which tend to restore the initial structure. The radial distribution functions are shown in Fig. 9.

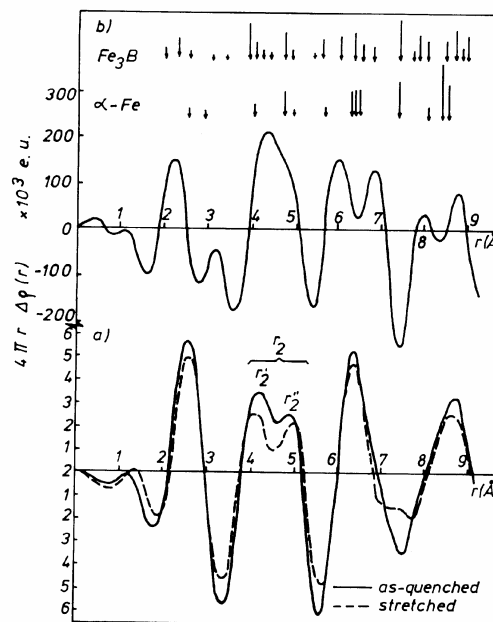


Fig. 9. The radial distribution functions for the $\text{Fe}_{80}\text{B}_{20}$ glassy ribbon. (a) Reduced RDF before and after deformation. (b) Differential RDF: (as-quenched state)– (stretched state).

If one compares the positions of the main maxima and minima in the differential RDF with the positions of the atomic coordination spheres of crystalline bcc iron and of the crystalline compounds FeB , Fe_2B , Fe_3B and Fe_4B , one concludes that the initial as-quenched states characterized by a higher level of SRO of the type Fe_3B than the plastically deformed state. The peak situated at ~ 0.22 nm speaks in favour of a dominant concentration of Fe-B pairs in the as-quenched state. The minima situated in the positions corresponding to the coordination spheres of

bcc α -Fe clearly indicate that in the plastically deformed state, an ordering similar to that occurring in crystalline α -Fe appears.

It is remarkable that the SRO of the type α -Fe, revealed in the sample deformed under tensile load is identical to the SRO of the stable crystalline phases which appear during crystallization of the amorphous $\text{Fe}_{80}\text{B}_{20}$ [32], i.e. α -Fe and tetragonal Fe_3B .

In conclusion, the deformation at room temperature (well below T_g) lead to a more disordered structure which occurs as a consequence of a greater compositional disorder. Fe_3B is a strongly bonded compound and, therefore, its formation is energetically favourable. The α -Fe precipitates as a consequence of the viscous flow of the glassy material. Uniaxial tensile load applied to the metallic glass induces profound modifications in the atomic short range order.

In amorphous $\text{Fe}_{80}\text{B}_{20}$, a compositional splitting was observed. This cannot avoid the modification of the medium range order whose extension depends on the ordering characteristic of SRO configurations. There is evidence of a bcc SRO characteristic to α -Fe and a SRO characteristic to Fe_3B . The observed effects can be correlated with the decrease of the corrosion resistance of the glassy metallic alloys subjected to high deformations.

The behaviour of the metglass during annealing was studied by Waseda [33] and modelled by Popescu [34]. The careful analysis of the glassy Pd_4Si has evidenced in the diffraction pattern a small but significant effect. The second diffraction maximum which is splitted changes the intensity of both component in different directions: the peak of larger intensity slightly increases and that of low intensity (visible as a pronounced kink) slightly decreases. This behaviour has been explained only by modelling of the structure in the frame of a model (DRPSU- dense random packing of structural units). A special process of relaxation has been applied in a computer array (160 atoms), based on the minimization of the free energy of the model. In this process the atoms were allowed to change their coordination spheres and bonding with the neighbouring atoms, if the modifications of bonding determine the diminishing of the total free energy of the model. The state of order was significantly improved after several iterations. The structural characteristics of the model for the case of relaxation without changing the coordination spheres were compared to those of the fully relaxed model (when the interatomic bonds were allowed). Fig. 10 shows the results.

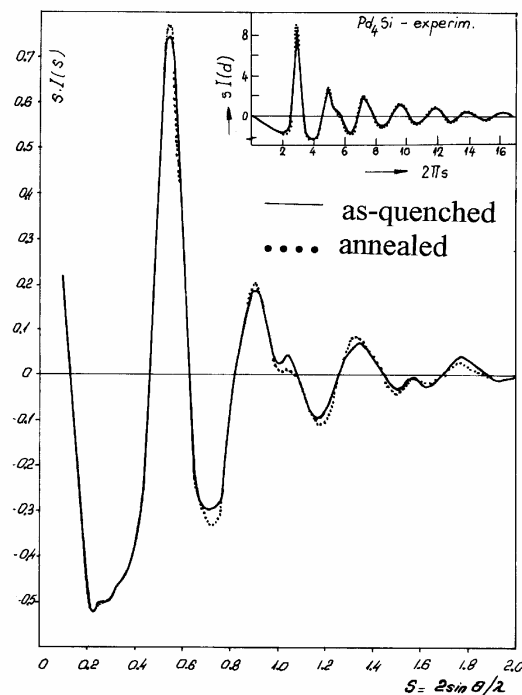


Fig. 10. The reduced radial distribution function for glassy Pd_4Si . The experimental results and the curve calculated from the DRPSU model. — initial relaxed configuration; --- final relaxed configuration (annealed) experimental: — as-quenched --- annealed, 250 °C, 40 min.

It is quite impressive how this small model can reproduce with high accuracy the fine details seen on the diffraction patterns and the modifications induced by annealing in the Pd₄Si glass. But, the greatest importance of the model is the possibility to understand directly what kind of transformations at the atomic scale are related to the thermal effect in glassy metallic alloys. Careful analysis of the model lead to the conclusion that the thermal relaxation is characterized by the rearrangement of the bond configuration so that the first coordination of metal and metalloid become narrower and the coordination polyhedra change their shapes toward the ideal ones known from the crystals. The improvement of SRO during annealing has a significant impact on MRO which extends toward larger distances. It is not yet possible to determine the level of extension of MRO by using only one model, but we think that in the future the simulation experiments will be able to give the answer to this question.

If the changes during annealing and tensile loading are so important and so different as regarding the effects produced in the metallic glassy alloys, then it is not impossible that the action of these factors upon a metglass ribbon give rise to an anisotropic ordering of the basic configurations that gives MRO. This means that the extended ordering (MRO) in glasses can be used to create anisotropy. In this case the metglass ribbons are good candidates for the investigation of the anisotropic effects, because they are quenched on a copper drum and, in the process of cooling the thermal gradient along the ribbon is very high while in the transverse direction is practically zero. Recently we have measured by X-ray diffraction the structure of a Fe₄₀Ni₄₀B₁₄P₆ ribbon of 1.5 centimeter width. The measurements has been performed for two orientations of the ribbon. The first one is parallel to the X-ray beam and the second one is transversal to the beam (the sample is rotated by 90°). The RDF were carefully processed and the final curves were compared (Fig. 11).

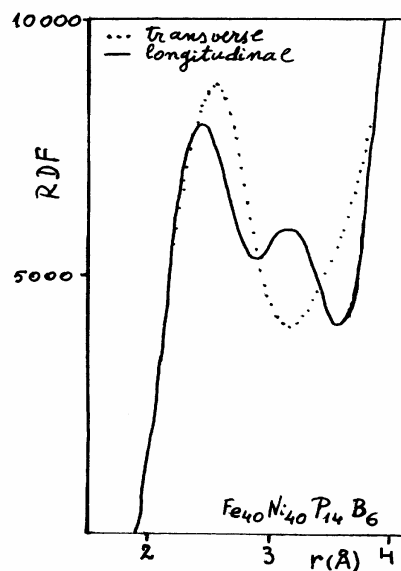


Fig. 11. The region of the first coordination sphere in the radial distribution function calculated from the diffraction pattern measured on a metglass ribbon of composition Fe₄₀Ni₄₀B₁₄P₆ in two positions: longitudinal and transversal in relation to the direction of the X-ray beam.

The results are highly surprising because the RDFs differ significantly from one direction of measurement to the other. The effect was confirmed by measuring the sample on both faces. For the transversal position the first coordination seems to be very uniform and homogeneous, while for the longitudinal position of the sample a coordination splitting occurs. These differences are preserved also for the second large coordination sphere where similar play between a pair of peaks persists. Now is not entirely clear what happens but, undoubtedly, the anisotropic change in SRO is

demonstrated (first coordination sphere changes) and anisotropic change in MRO is revealed (the second and higher coordination spheres are modified).

It is important to look on the possibility to have MRO in the liquid state of the solid materials. In the last years much attention was paid to the investigation of the atomic-scale structure and of physical properties of liquid binary and multi-component alloys. The most results can be interpreted by taking into account the association phenomena, i.e. the formation of homo-atomic and hetero-atomic clusters. Hoyer and Jödicke [35] have shown that in golden rich Au-Ge alloys, stable MRO occurs up to nearly 650 K above the melting point. It was concluded that the alloys contain associated regions, possibly bearing some resemblance to the structure of metastable crystalline alloys. The experimental structure factor of the Au_4Ge in molten state is shown in Fig. 12. The most surprising feature on the curve is the small pre-peak situated on the left side of the main peak at $Q \sim 1.4 \text{ \AA}^{-1}$. This pre-peak has some resemblance with the pre-peak observed in covalent materials. Therefore, it can be ascribed to some kind of medium range order in the liquid and it is tempting to compare it with that observed in liquid As_2Se_3 . To have more insight into the structure of the alloy related to the pre-peak, the modelling of the atomic scale arrangement was performed in a frame of a model consisting of a big cluster built from tetrahedral Ge-Au₄ units. Thirty three tetrahedral units have been linked in a random manner. The cluster was relaxed by using appropriate force constants and a Monte-Carlo computer procedure [36]. The structure factor of the relaxed model has been calculated and compared to the experimental one (Fig. 13).

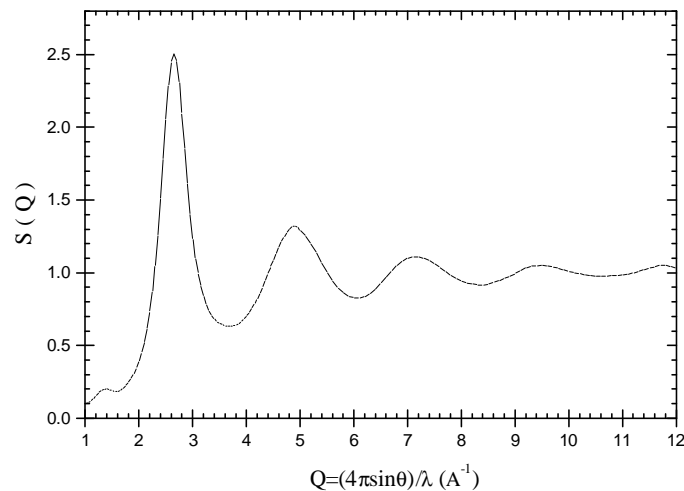


Fig. 12. The X-ray diffraction pattern (structure factor) of Au_4Ge molten alloy at 893 K (620 °C).

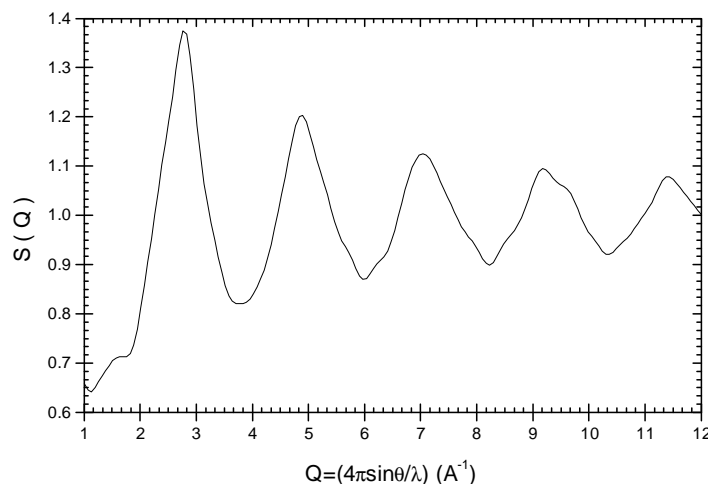


Fig. 13. The structure factor of the model with Ge-Au₄ heteroassociates (165 atoms) developed for the molten Au_4Ge alloy.

The model reproduces fairly well the pre-peak experimentally detected. The above results allow to conclude that the Au₄Ge alloy, in the molten state, exhibits some kind of medium range ordering as a packing of tetrahedral units of gold with a germanium atom in the centre. A relative ordering of these units can be produced as a result of cooling the melt just above the melting temperature. In the final stage a metastable crystalline phase can be produced by crystallization, as observed.

5. Conclusions

The medium range order is a challenging problem in solid state physics. There are systems with well developed MRO. For the covalent classes, especially for chalcogenide glasses, the MRO can be satisfactorily explained in the frame of the nanoparacrystallite theory. The change of MRO is related to the change of paracrystallites. In metallic glassy alloys the structural change under the action of tensile load or by annealing is reflected both in the short range order and in the medium range order, as opposite to covalent glasses where the short range order is usually preserved. The control of MRO is important because the properties of the materials depend strongly on the atomic scale order. The detailed characterization of MRO and its extension is still desirable. A better knowledge of the order peculiarities in non-crystalline solids will be rewarding, if the main goals of the material technology are considered: the improvement of the material properties and the creation of new materials.

References

- [1] M. Popescu, Proc. Intern. Conf. "Amorphous Semiconductors '78", Pardubice, Czechoslovakia, Vol. **1**, pag. 185 (1978).
- [2] J. C. Phillips, J. Non-Cryst. Solids **34**, 153 (1979).
- [3] G. Lucovski, F. L. Galeener, J. Non-Cryst. Solids **37**, 53 (1980).
- [4] S. R. Elliott, in Physics of Amorphous Materials, Longman, London, 2-nd edition, 1990.
- [5] S. R. Elliott, J. Non-Cryst. Solids **97&98**, 159 (1987).
- [6] M. V. Baidakova, N. N. Faleev, T. F. Mazets, E. A. Smorgonskaya, J. Non-Cryst. Solids **192&193**, 149 (1995).
- [7] A. H. Narten, C. G. Venkatesh, S. A. Rice, J. Chem. Phys. **64**, 1106 (1976).
- [8] M. Popescu, J. Non-Cryst. Solids **75**, 483 (1985).
- [9] A. L. Renninger, B. L. Averbach, Acta Crystallographica B, **29**, 1583 (1973).
- [10] R. Zallen, M. Slade, Phys. Rev. B, **9**, 1627 (1974).
- [11] L. E. Busse, S. R. Nagel, Phys. Rev. Lett. **47**(25), 1848 (1981).
- [12] L. E. Busse, Phys. Rev. B, **29**, 3639 (1984).
- [13] O. Uemura, Y. Sagara, D. Muno, T. Satow, J. Non-Cryst. Solids **30**, 155 (1978).
- [14] A. J. Apling, A. J. Leadbetter, A. C. Wright, J. Non-Cryst. Solids, **23**, 369 (1977).
- [15] S. R. Elliott, Phys. Rev. Lett. **67**(6), 711 (1991).
- [16] A. A. Vaipolin, E. A. Porai-Koshits, Fiz. Tverd. Tela (russ), **5**(1), 246 (1963).
- [17] R. Hosemann, Z. für Physik **128**, 1 (1950); **128**, 465 (1950).
- [18] M. Itoh, J. Non-Cryst. Solids **210**, 178 (1991).
- [19] A. M. Hindeloh, R. Hosemann, J. Mat. Sci. **26**, (1991).
- [20] A. J. Leadbetter, A. J. Apling, J. Non-Cryst. Solids **15**, 250 (1974).
- [21] J. P. de Neufville, S. C. Moss, S. R. Ovshinsky, J. Non-Cryst. Solids **13**, 191 (1974).
- [22] S. M. Sharma, S. K. Sikka, Progress in Mat. Sci. **40**, 1 (1996).
- [23] I. T. Penfold, P. S. Salmon, Phys. Rev. Lett. **67**, 97 (1991).
- [24] H. Badaczek, Polymeric Materials Encyclopedia, CRC Press Inc., p. 4875, 1996.
- [25] T. Matsumoto, R. Maddin, Acta Met. **19**, 725 (1971).
- [26] R. Maddin, T. Matsumoto, Mater. Sci. Eng. **9**, 153 (1972).
- [27] C. A. Pampillo, H. S. Chen, Mater. Sci. Eng. **13**, 181 (1974).
- [28] T. Masumoto, R. Maddin, Mater. Sci. Eng. **19**, 1 (1975).
- [29] T. Masumoto, H. Kimura, A. Inoue, Y. Waseda, Mater. Sci. Eng. **23**, 141 (1976).
- [30] Y. Waseda, T. Egami, J. Mater. Sci. **14**, 1249 (1979).

- [31] M. Popescu, J. Non-Cryst. Solids **169**, 155 (1994).
- [32] T. Kémény, I. Wincze, B. Fogarassy, Sigurd Arajs, Phys. Rev. B, **20**, 476 (1979).
- [33] Y. Waseda, W. A. Miller, phys. stat. sol. (a), **49**, k31 (1978).
- [34] M. A. Popescu, J. de Physique, Coll. C8, suppl. No.8, Tome **41**, C8-309, (1980).
- [35] W. Hoyer, R. Jödicke, J. Non-Cryst. Solids, **192&193**, 102 (1995).
- [36] W. Hoyer, M. Popescu, F. Sava, A. Lörinczi in “Homage Book – Andrei Andriesh”, M. Popescu editor, INOE&INFM Publishing House, Bucharest, Romania, p. 185, 1999.

Examples: Non-crystalline materials. Here you will find a cross-section of PDF studies carried out on the beamline. Experiments were carried out on ID22 (since 2014), and ID31 (2002 - 2013). Combining Rietveld analysis with PDF analysis can be advantageous for crystalline materials with short-range order representing deviations from the average (crystallographic) structure. Thus the structural properties of semiconducting nanoparticles of selenium grown in the pores of a neodymium zeolite-Y were investigated using this approach [2]. Powder diffraction patterns were measured at 41 keV (0.298 Å...) up to 110° in 2θ , and the average structure refined, which included three Se sites forming a cluster in the large (13 Å... diameter) cavity of. Non-crystalline materials are thus by definition disordered in some respect of their structure. Unfortunately, order/disorder can not be precisely defined for non-crystalline materials and usually rests on determining what degree of order can be identified experimentally at different length scales. Four generic scales can be identified (Wright 1994). Although medium-range order is believed to play an important role in determining many of the physical-mechanical properties of solid disordered materials (Elliot 1983), both its physical nature and influence on such properties is still however poorly understood. Indeed, the relationship between short- and medium-range order varies between material systems. Short Range Order Radial Distribution Function Chalcogenide Glass Medium Range Order Amorphous Selenium. Lucovsky, G. (1987) Specification of medium-range order in amorphous materials, J. Non-Cryst. Solids 97 & 98, 155-158. CrossRef Google Scholar. 2. Ervinka, L. (1987) Comments on medium-range ordering in non-crystalline solids, J. Non-Cryst. Solids 97 & 98, 191-223. Google Scholar. 11. Medium-range order and random networks. Journal of Non-Crystalline Solids, Vol. 293-295, Issue. , p. 146. CrossRef. Google Scholar. Designing intermediate-range order in amorphous materials. Nature, Vol. 419, Issue. 6905, p. 381. Medium-range order in alkali metaphosphate glasses and melts investigated by reverse Monte Carlo simulations and diffraction analysis. Physical Review B, Vol. 67, Issue. 10 Journal of Non-Crystalline Solids 438 (2016) 10-17. Contents lists available at ScienceDirect. Journal of Non-Crystalline Solids. journal homepage: www.elsevier.com/locate/jnoncrysol. Medium range structural order in amorphous tantalum spatially resolved. with changes to atomic structure by thermal annealing. Martin J. Hart. Keywords: Amorphous materials Fluctuation electron microscopy Nanodiffraction Medium-range order Tantalum-pentoxide Internal friction. abstract. Amorphous tantalum (α -Ta₂O₅) is an important technological material that has wide ranging applications in electronics, optics and the biomedical industry.